scientific reports

Check for updates

OPEN

Mechanism of antibacterial and antibiofilm of thiazolidinone derivative TD-H2-A against *Staphylococcus aureus*

Bingyu Du[1,5], Fen Xue[1,5], Hui Xu[1], Rui Zhao[2], Tiantian Zhang[1], Shiqing Han[3], Tao Zhu[4]✉, Yefei Zhu[1]✉ & Yanfeng Zhao[1]✉

Staphylococcus aureus **is one of the most common pathogens causing widespread infections. It has been demonstrated that thiazolidinone derivative (TD-H2-A), a small molecule compound that targets WalK protein through high-throughput screening, exerts antibacterial and anti-biofilm effects on *S. aureus*. In this study, we further ascertained the impact of TD-H2-A on biofilms at different stages. The phosphorylation assay and RNA sequencing were carried out to elucidate the underlying mechanism. The results revealed that TD-H2-A inhibited WalK autophosphorylation, implying that the antibacterial effect of TD-H2-A may be achieved by inhibiting the activity of WalK. The transcriptome analysis showed that TD-H2-A treatment induced 994 differentially expressed genes (DEGs), of which, 481 were upregulated and 513 were downregulated. Kyoto Encyclopedia of Genes and Genomes (KEGG) enrichment analysis revealed that 43 among 58 genes involved in ribosome synthesis were upregulated, and the transcript levels of the genes responsible for membrane transport were altered significantly. According to our research, TD-H2-A has an antibacterial mechanism with multitarget and multipathway. This study provided new ideas for the development of new drug target screening against *S. aureus* infections.**

Keywords *Staphylococcus aureus*, WalK, RNA-seq, TD-H2-A

Staphylococcus aureus, one of the most common human pathogens, can cause an extensive range of illnesses, ranging from simple skin infections to major tissue infections and sepsis, depending on the invasion site, extent, and the immune status of the host[1,2]. *S. aureus* is the second-most prevalent pathogen among hospital-acquired pneumonia cases. In Europe, 29.9% of *S. aureus* isolates were resistant to oxacillin[3,4]. Owing to antibiotic resistance and the lack of a viable vaccination, treatment of *S. aureus*, especially methicillin-resistant *S. aureus* (MRSA) infections, has become more difficult and complicated[5].

The formation of biofilms further complicates the treatment of *S. aureus* infections. Bacteria embedded in a biofilm are in a low metabolic state or a stable growth phase, which is difficult to be penetrated by host defense molecules and antibiotics. They can resist the host's immune response and escape killing by antibiotics. Their resistance to antimicrobial agents can be 10 to 1000 times higher compared to their planktonic lifestyle[6–9]. Biofilms lead to the development of a persistent infection that is less susceptible and more resistant to environmental stimuli. Biofilms are, therefore, an important target for the treatment of infections.

Bacteria utilize two-component signaling systems (TCSs) to perceive and respond to environmental changes, which are crucial for the adaptation of pathogenic bacteria to their host environment[10]. Among the 17 TCSs identified in *S. aureus*, WalKR (YycFG) stands out as the sole TCS essential for bacterial viability[11]. The WalK/R signal transduction system has been demonstrated to regulate key cellular processes, including cell membrane metabolism, cell wall synthesis, and biofilm formation in *S. aureus*[10,12]. After stimulation by the external environment, the histidine protein kinase WalK is autophosphorylated, and the phosphate group is transferred

[1]Laboratory Medicine Center, The Second Affiliated Hospital, Nanjing Medical University, Nanjing, People's Republic of China. [2]Department of Clinical Microbiology, Shanghai Centre for Clinical Laboratory, Shanghai, People's Republic of China. [3]College of Biotechnology and Pharmaceutical Engineering, Nanjing Tech University, Nanjing, People's Republic of China. [4]Department of Medical Microbiology and Immunology, Wannan Medical College, Wuhu, People's Republic of China. [5]Bingyu Du and Fen Xue contributed equally to this work and share the first authorship. ✉email: zhutao@wnmc.edu.cn; zhuyf@njmu.edu.cn; zhaoyanfeng@njmu.edu.cn

to the cognate response regulator WalR. Phosphorylated WalR binds to the promoter region of the target genes and modulates their expression[13].

Previously, we found that thiazolidinone derivative (TD-H2-A), a small molecule compound obtained via high-throughput screening to target the WalK protein, possesses excellent bactericidal as well as antibiofilm activity against *S. aureus* ATCC 35556 both in vitro and in vivo[14]. However, the mechanisms underlying this process remain unknown. In this study, we further ascertained the impact of TD-H2-A on biofilm development, in addition, TD-H2-A was confirmed to inhibit the phosphorylation of His-WalK' via an in vitro phosphorylation inhibition assay with purified recombinant proteins. RNA-seq is a powerful tool for analyzing the adaptability of bacteria under antibiotic selection pressure, elucidating the mechanism of antibiotics action, and identifying novel drug targets[15]. Therefore, we sought to investigate the antibacterial and antibiofilm mechanisms of TD-H2-A against *S.aureus* using RNA-seq.

Results

Effect of TD-H2-A on *S. aureus* ATCC 35,556 biofilms

In previous study, we found that TD-H2-A (Figs. S1–S4) had potent bacteriocidal activities toward cells in mature biofilms by assessing the inhibitory and bacteriocidal activities of it against *S. aureus* embedded in mature biofilms[14]. In order to better understand the impact of TD-H2-A on the *S. aureus* biofilm at various stages, we used Scanning electron microscopy (SEM) to study the effects of TD-H2-A on the biofilm development during the initial attachment and the maturation phase. As illustrated in Fig. 1, on the initial attachment phase (6 h), SEM images reveal that untreated cells exhibit pronounced biofilm formation on the glass surface. Vancomycin demonstrated an inhibitory effect on bacterial biofilms. In contrast, upon 5×MIC TD-H2-A treatment, we noticed that some cells presented rough and shrunken surfaces. TD-H2-A at 5×MIC significantly decreased cellular aggregation on glass surfaces. In TD-H2-A treated group, *S. aureus* biofilms also showed a decrease at the maturation phase (48 h).

Inhibition assay for walk part autophosphorylation

To confirm whether TD-H2-A inhibited the autophosphorylation activity of the WalK, we performed an in vitro phosphorylation assay using a commercially available recombinant *S. aureus* WalK (Lys208-Glu608) protein with an N-His tag. This assay utilized an ATP kit that quantitatively measures light produced by luciferase-catalyzed enzymatic reactions. The remaining ATP amount is inversely proportional to kinase activity; higher kinase activity results in less ATP and lower luminescence, while higher luminescence indicates more remaining ATP. As shown in Fig. 2, we assessed the His-WalK' protein's ability to undergo autophosphorylation. The luminescence value significantly decreased with the addition of His-WalK', indicating that WalK indeed has autophosphorylation activity. Next, we examined the effect of TD-H2-A on the autophosphorylation of the His-WalK' protein. The luminescence value was resorted to the level comparable to ATP control group after the drug

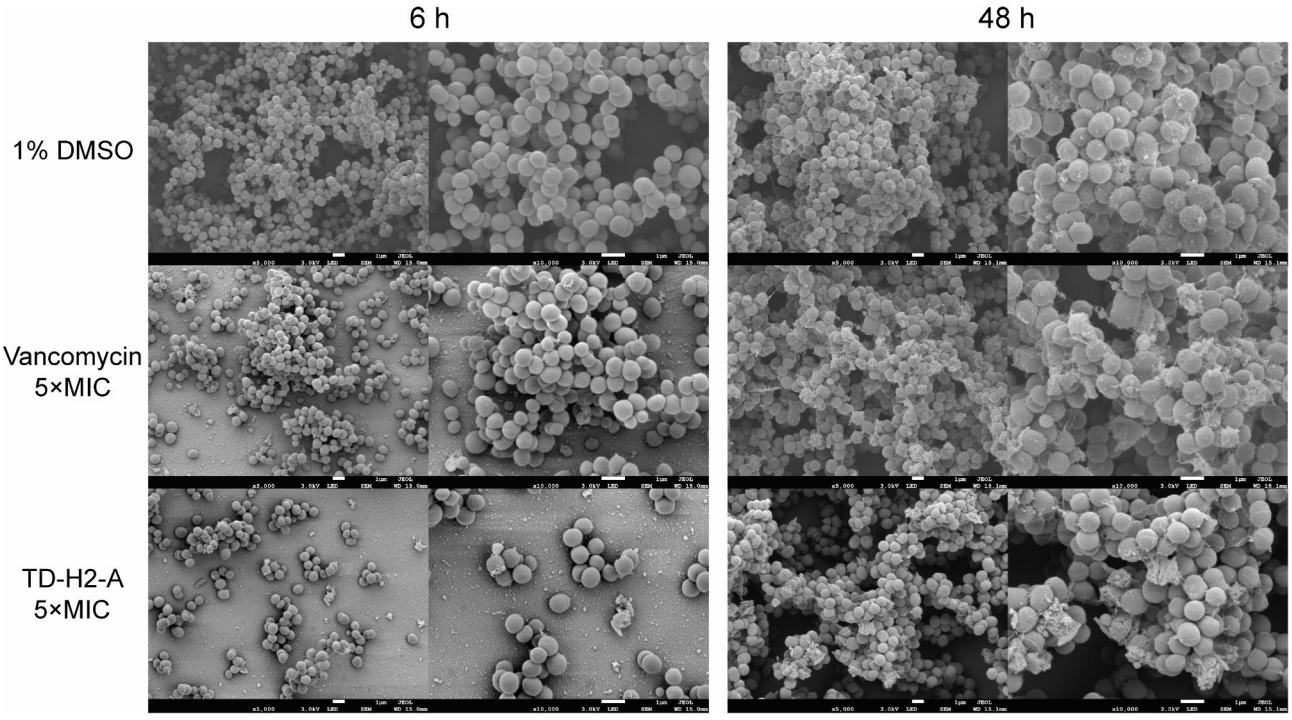

Fig. 1. SEM observation of the effect of different inhibitory concentration of TD-H2-A on *S.aureus* ATCC 35,556 biofilms structure at the initial attachment phase (6 h) or the maturation phase (48 h). SEM images of biofilms taken at ×5,000, ×10,000 magnification, respectively.

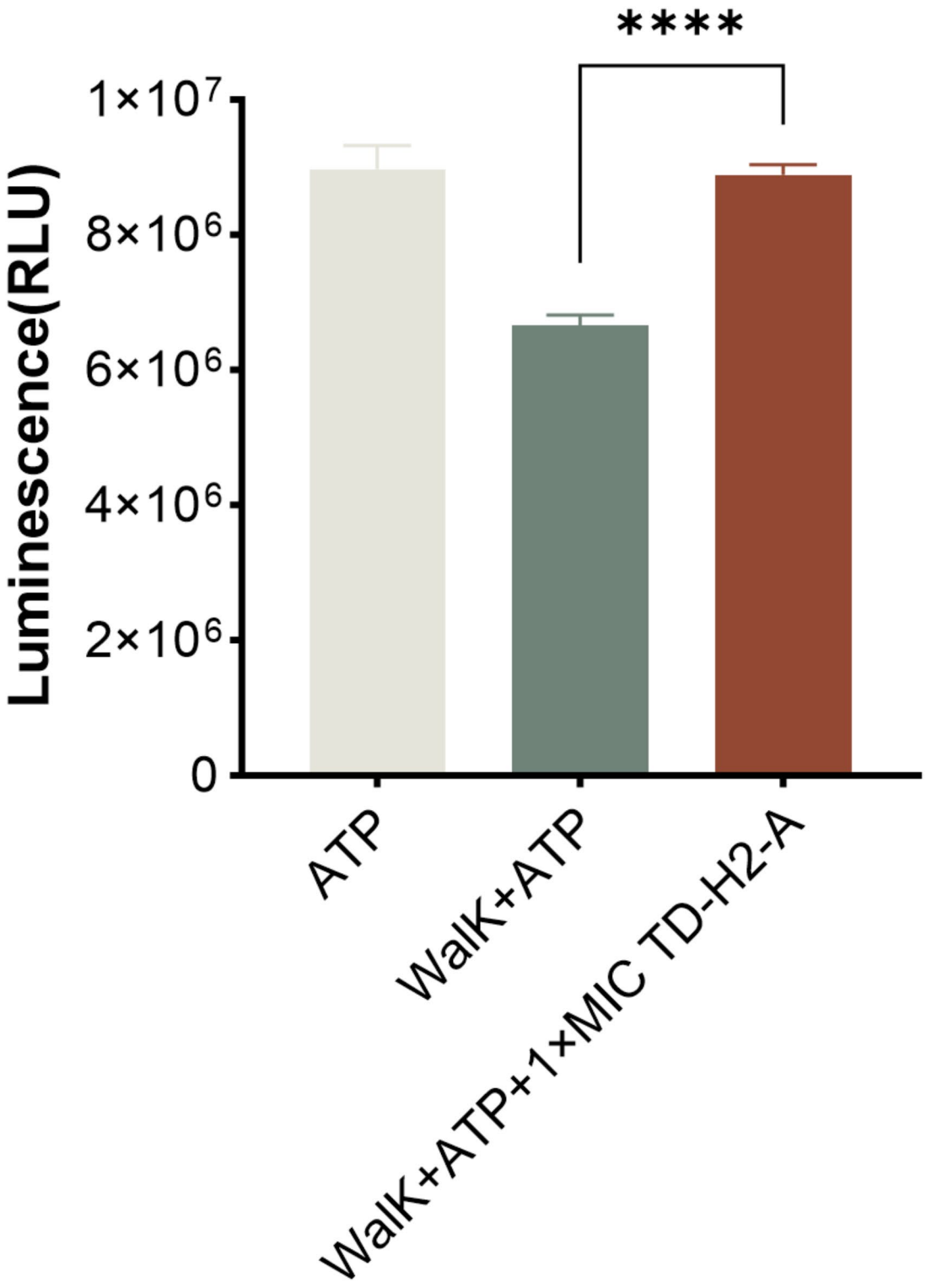

Fig. 2. The reaction system was composed of 4 μg His-WalK' protein and 4 μM ATP, without His-WalK' protein served as control. The effect of TD-H2-A on the His-WalK' protein phosphorylation. All experiments were performed with three biologically independent experiments, and the mean ± SD is shown, **** indicates $p < 0.0001$.

molecular was supplemented to reaction mixture, suggesting that TD-H2-A inhibited the autophosphorylation of the His-WalK' protein.

Differential expression analysis

In order to investigate the antibacterial mechanism of TD-H2-A in further detail, we used RNA-seq to conduct a transcriptome study. Between the TD-H2-A-treated group and the 1% DMSO control group, the gene expression analysis revealed a total of 994 significantly DEGs, of which 481 were downregulated, and 513 were upregulated (Fig. 3). The top 15 upregulated DEGs (Table 1) were mainly genes related to drug efflux pumps in *S. aureus*, such as *mepA*, *mepB*, and *mepR* (multidrug efflux MATE transporter MepA, MepB and MepR), *farE* (fatty acid efflux MMPL transporter FarE), *vraD*, and *vraE* (peptide-resistance ABC transporter permease subunit).

Quantitative reverse transcription polymerase chain reaction (qRT-PCR) validation of selected DEGs

To verify the RNA-seq results, we randomly selected ten genes *ndk*, *ugpC*, *gntK*, *sdpB*, *ftsL*, *ytkD*, *sdrC*, *sdrD*, *vraD*, *vraE* from the DEGs to detect their expression by qRT-PCR on the same samples. As shown in Fig. 4, the DEGs validation results were consistent with the RNA-seq analysis, indicating that the RNA-seq analysis in this work was highly accurate and reliable.

Gene ontology (GO) and KEGG enrichment analysis of DEGs

The GO classification was performed according to molecular function, biological process, and cellular component; the top 10 GO term items with the smallest P-value, namely the most significant enrichment in each GO classification, were selected, including rRNA binding, structural constituent of ribosome, ribosomal subunit and so on (Fig. 5A). With the results of KEGG enrichment, the degree of enrichment was measured by the Rich factor, False discovery rate (FDR) values, and the number of genes enriched by this pathway. The top

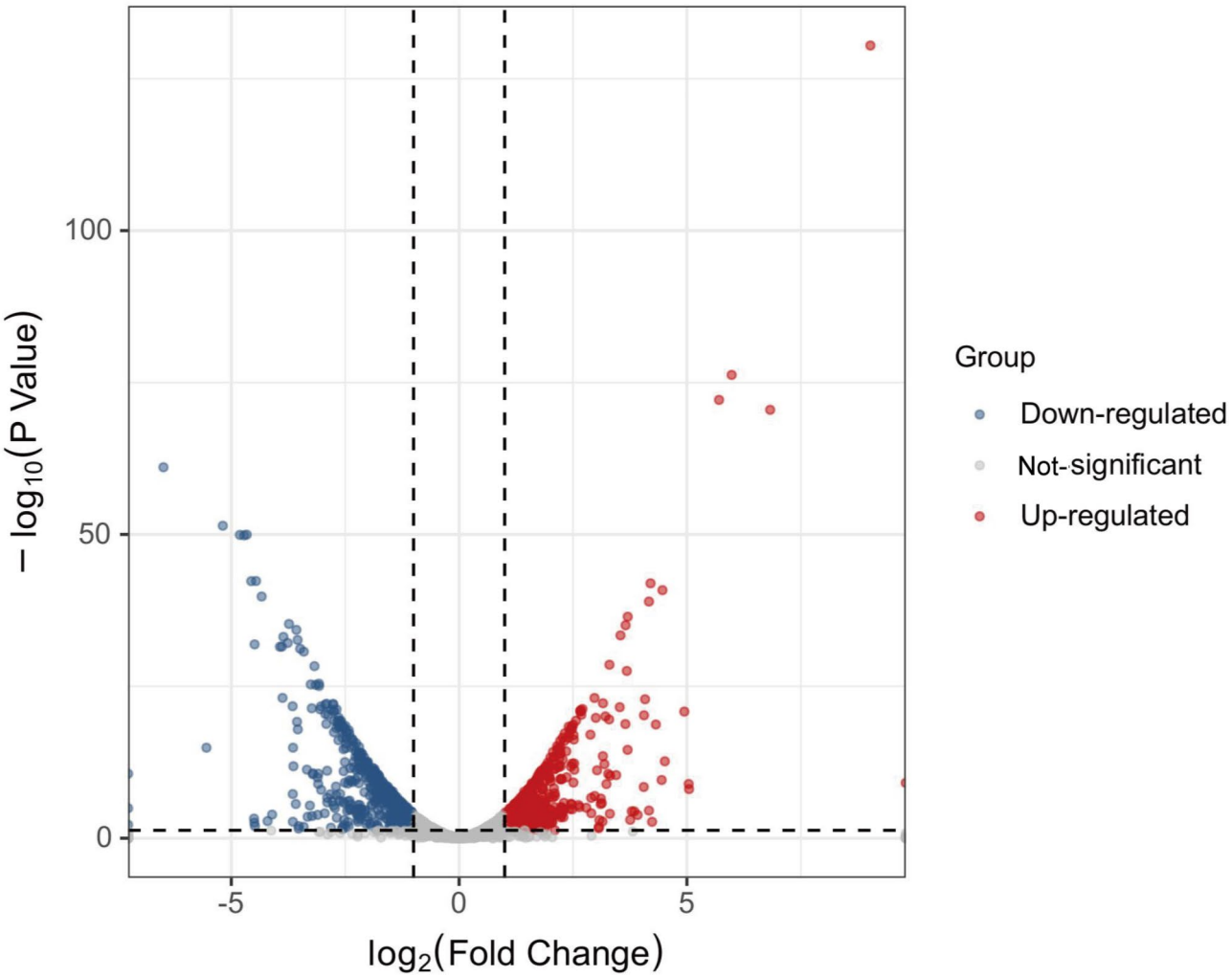

Fig. 3. Volcano plot of DEGs. The two vertical dashed lines are the 2-fold expression difference threshold, and the horizontal dashed line is the $P = 0.05$ threshold. Red dots indicate the upregulated genes, blue dots indicate the downregulated genes and gray dots indicate non-significant DEGs.

Gene-ID	Gene	Product	TD-H2-A vs. 1%DMSO Log_2Fold Change
SAV_RS01855	*mepA*	Multidrug efflux MATE transporter MepA	9.03
SAV_RS01860	–	MepB family protein	6.83
SAV_RS01850	*mepR*	Multidrug efflux MATE transporter transcriptional repressor MepR	5.98
SAV_RS13920	*farE*	Fatty acid efflux MMPL transporter FarE	5.71
SAV_RS14200	–	Aspartate aminotransferase family protein	5.05
SAV_RS14015	–	PTS transporter subunit IIC	5.04
SAV_RS14730	*vraD*	Peptide resistance ABC transporter permease	4.94
SAV_RS07225	–	Hypothetical protein	4.52
SAV_RS05285	*clpB*	ATP-dependent chaperone ClpB ubunit	4.46
SAV_RS13690	–	DUF2188 domain-containing protein	4.45
SAV_RS11215	*ilvD*	Dihydroxy-acid dehydratase	4.32
SAV_RS05580	–	YxeA family protein	4.23
SAV_RS14735	*vraE*	Peptide resistance ABC transporter permease subunit	4.20
SAV_RS01210	–	M23 family metallopeptidase	4.17
SAV_RS12940	–	YhgE/Pip domain-containing protein	4.17
SAV_RS13085	–	Hypothetical protein	− 6.49
SAV_RS07905	*ndk*	Nucleoside-diphosphate kinase	− 5.55
SAV_RS01215	*ugpC*	sn-glycerol-3-phosphate ABC transporter ATP-binding protein UgpC	− 5.19
SAV_RS07145	–	Hypothetical protein	− 4.81
SAV_RS13675	–	GntR family transcriptional regulator	− 4.72
SAV_RS13670	*gntK*	Gluconokinase	− 4.66
SAV_RS01100	–	DUF871 domain-containing protein	− 4.56
SAV_RS01755	–	N-acetylneuraminate lyase	− 4.50
SAV_RS13630	*sarU*	HTH-type transcriptional regulator SarU	− 4.49
SAV_RS06985	–	Aquaporin family protein	− 4.49
SAV_RS07090	–	Hypothetical protein	− 4.48
SAV_RS01585	–	CHAP domain-containing protein	− 4.46
SAV_RS12615	*sdpB*	CPBP family intramembrane metalloprotease SdpB	− 4.33
SAV_RS07900	–	Hypothetical protein	− 4.20
SAV_RS05610	–	TM2 domain-containing protein	− 4.10
SAV_RS04090	–	Threonine/serine exporter ThrE family protein	− 3.93

Table 1. The top 15 up- and down—regulated DEGs.

20 KEGG pathways with the smallest FDR values and the most significant enrichment terms were selected for display, including ribosome, ABC transporters, Lysine biosynthesis and so on. The results are shown in Fig. 5B.

Functional analysis of differentially expressed genes

Our previous study demonstrated that TD-H2-A has an inhibitory effect on the mature biofilms of *S. aureus*. As shown in Fig. 6, TD-H2-A also affects the transcription of genes involved in biofilm formation in *S. aureus*. In addition, the expression of numerous 50 S ribosomal protein and 30 S ribosomal protein genes were found to be upregulated in the TD-H2-A treatment (Fig. 7A), indicating that the translation capacity of *S. aureus* was significantly improved after the TD-H2-A treatment.

Furthermore, according to the sequencing data and bioinformatics analysis, the differentially expressed genes were those involved in membrane transport. They mainly encode ABC transporters protein, the phosphotransferase system (PTS), and the bacterial secretion system (Fig. 7B). The present findings are in line with previous ones[14], implying that TD-H2-A influences the cell membrane permeability of *S. aureus*.

Discussion

The present time is witnessing a global health crisis as a result of the rise in antibiotic resistance and the decline in the discovery of new antibiotics[16]. Multidrug-resistant *S. aureus* has become one of the major causes of nosocomial and community-acquired infections. Thus, it is extremely urgent to explore innovative and highly efficient antibacterial agents with novel antimicrobial modes of action in response to bacterial drug resistance.

The two-component system WalKR is essential for cell viability, and it plays a role in *S. aureus* virulence. The knockout strain of this system was not successfully constructed by homologous recombination[17,18]. Standard treatments for multidrug-resistant *S. aureus* infections include vancomycin, linezolid, daptomycin, and beta-lactams[19]. The WalK mutation was detected in both vancomycin- and daptomycin-resistant strains[20,21]. This finding also indicates that the WalK histidine kinase is a promising antibacterial target. We hypothesize that the thiazolidinone derivative interacts with *S. aureus* WalK-HK to exert its bactericidal effect. Drug molecules

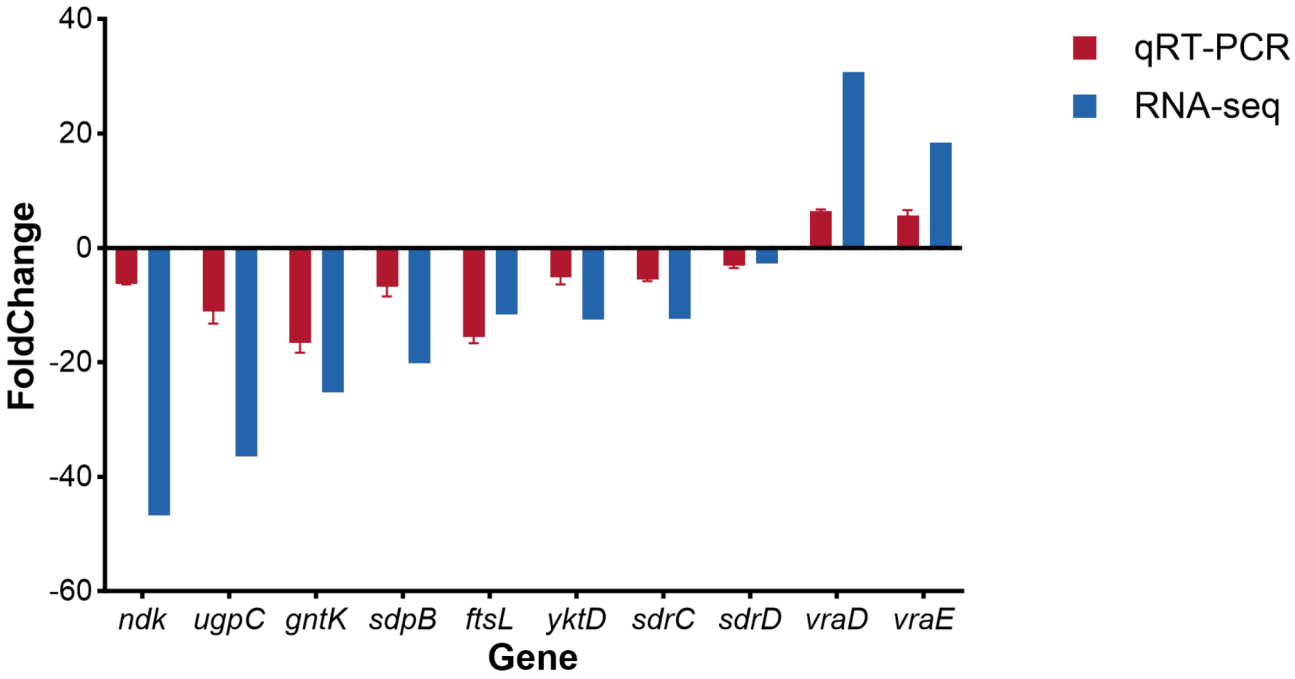

Fig. 4. Validation of DEGs in *S. aureus* ATCC 35,556 treated with TD-H2-A using qRT-PCR. All assays were performed with three biologically independent experiments, and the mean ± SD is shown.

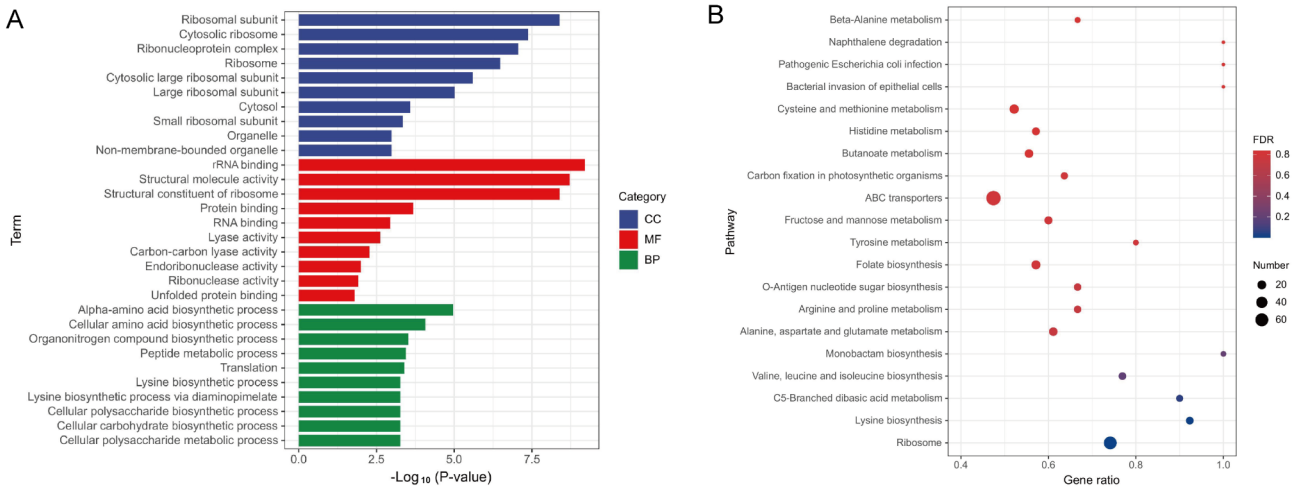

Fig. 5. (A) GO enrichment results for DEGs, (B) KEGG enrichment results for DEGs.

are more likely to bind in the CA domain, which results in blockade of ATP binding. Using an in vitro phosphorylation inhibition assay, we found that TD-H2-A inhibits the auto-phosphorylation of the His-WalK' protein. However, we are unable to complete the TD-H2-A in vitro binding experiment as the amount of the recombinant protein we obtained was limited.

An ideal antibiotic would be hard to develop resistance. Despite the fact that antibiotics that are not prone to induce resistance are attractive clinically, the most common method for characterizing mechanisms of action (MOA) is to select resistant mutants. This makes it a major challenge to investigate the antimicrobial mechanisms of new antibiotics without resistant mutants[16]. The minimum inhibitory concentration (MIC) of TD-H2-A for *S. aureus* HG001 isolate was 6.5 μg/mL. In the previous resistance experiment, TD-H2-A did not led bacteria to develop drug resistance, and no mutations in the *walK* gene were detected in the sequencing results[14]; thus, WalK could not be identified as the only target of TD-H2-A. The antibacterial and antibiofilm activities of TD-H2-A may be due to a multifactorial mechanism.

Subsequently, we performed transcriptome analyses to unveil the underlying mechanisms of TD-H2-A action on *S. aureus*. Surface attachment is the first stage of biofilm formation. At this stage, the planktonic staphylococcal cells attach to biotic or abiotic surfaces. During infection, *S. aureus* mainly encounters biological

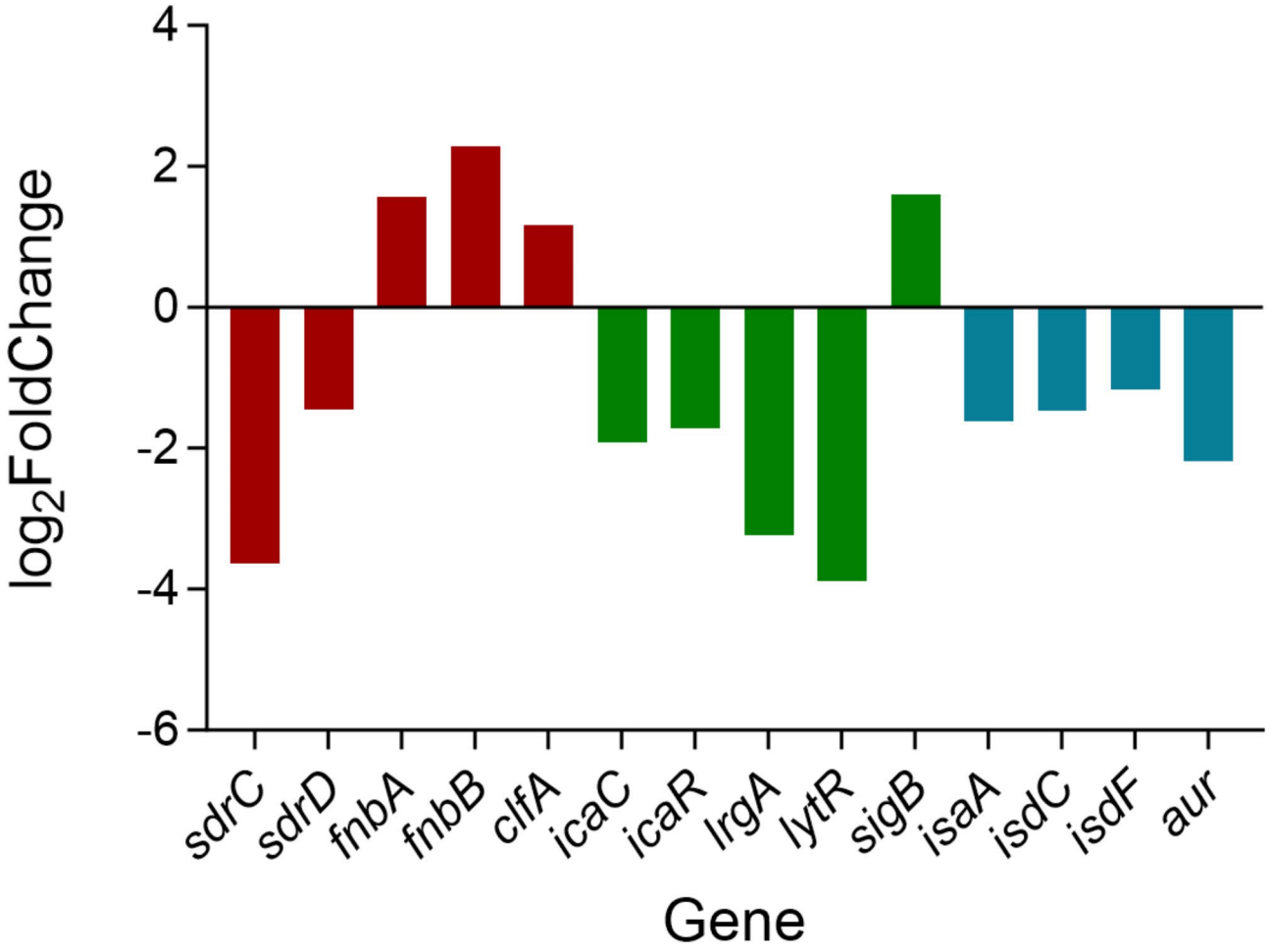

Fig. 6. DEGs associated with the biofilm.

surfaces covered with the host's matrix, including fibrinogen, fibronectin, vitronectin, and collagen. Cell-wall-anchored proteins, the best-characterized members of the microbial surface components that recognize adhesive matrix molecules (MSCRAMMs), facilitate binding to these biotic surfaces[22]. Some MSCRAMMs are believed to promote biofilm formation by mediating initial attachment to host matrix components, which include the serine-aspartate repeat protein family (SdrC and SdrD)[23,24]. Except for the abovementioned interactions with the components of the host matrix, SdrC could also promote *S. aureus* to attach to abiotic surfaces[25,26]. The *sdrC* and *sdrD* genes were significantly downregulated in the TD-H2-A-treated group.

The attached bacteria then multiply and form microcolonies on the surface. In the next stage, these microcolonies develop into distinct structures and form a biofilm. Cell proliferation into clusters and the further formation of biofilm layers are mediated by the production of intercellular polysaccharide adhesin, which constitutes the major component of the staphylococcal biofilm and is synthesized by proteins encoded by *icaADBC*[27,28]. The downregulation of *icaC* demonstrated that TD-H2-A attenuates *S. aureus* microcolony aggregation. Biofilm formation is a social group behavior, and every step, from the initial attachment to the dissemination of the mature biofilm, is strictly regulated[29]. In this experiment, the expression levels of some genes related to the regulation of biofilm formation in *S. aureus* were changed, including *lytR*, *lrgA* (encoding murein hydrolase regulator), *sigB* (encoding RNA polymerase sigma factor), and *isaA*.

Compared to the untreated growth group, a large number of genes related to membrane transport were differentially transcribed in the TD-H2-A-treated group, including ABC transporters, the phosphotransferase system (PTS), and the bacterial secretion system. Numerous studies have confirmed that the ABC transport system is responsible for bacterial nutrient uptake and efflux of toxins and antibiotics, as well as playing a potentially pathogenic role in infection of the host[30]. Furthermore, genes encoding proteins associated with the PTS transport system were found to be altered in the presence of TD-H2-A. PTS generally phosphorylates various sugars and their derivatives via phosphocascade and then transports them into the cell[31]. In addition, the inhibition of the PTS transport system is associated with retarded bacterial growth[32]. ABC transporters have been discovered to influence the lipid makeup of the membranes in which they are lodged, in addition to their notable impacts on drug efflux[33–35]. In previous research, using the LIVE/DEAD™ BacLight™ Bacterial Viability Kit for microscopy and quantitative assays, we found that TD-H2-A treatment could increase the membrane permeability of *S. aureus*[14].

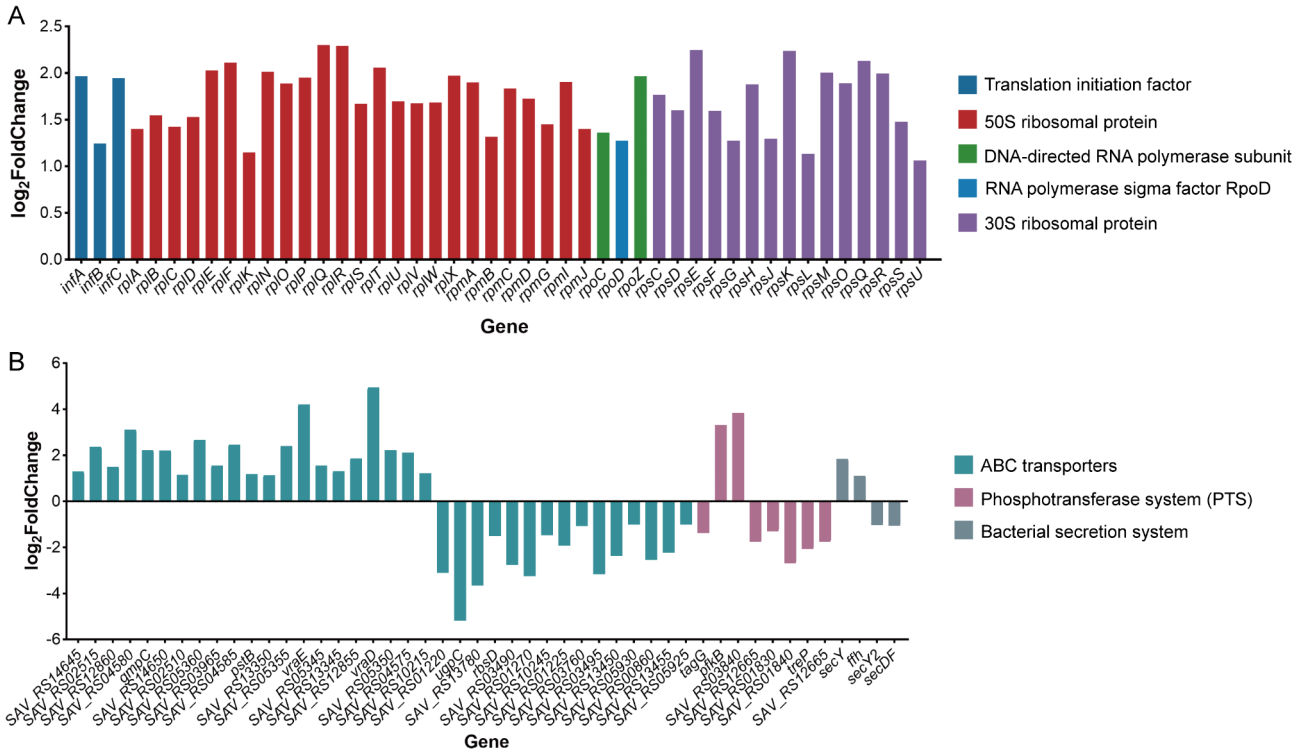

Fig. 7. (A) DEGs associated with the ribosome. (B) DEGs associated with cell membrane permeability.

We found that there might be another distinct MoA contributing to TD-H2-A's antimicrobial action in addition to membrane perturbation. GO and KEGG enrichment analysis revealed that treatment by TD-H2-A led to remarkable upregulation of numerous genes encoding 50 S ribosomal subunits and 30 S ribosomal subunits, which were all enriched in the ribosome pathway. Ribosomes, which translate genetic information into amino acid sequences, are critical organelles for the survival and growth of bacteria[36]. The bacterial ribosome is one of the most important targets of antibacterial agents. So far, approximately 60% of the approved antibacterial agents work by targeting ribosomes[37]. Research proves that peptidomimetic antibiotic 10 showed potent killing of multiple drug-resistant gram-negative bacteria, KEGG enrichment analysis revealed that treatment by 10 led to large up-regulation of numerous genes encoding 70 S ribosomal subunits that all were enriched in the ribosome pathway. Additional in vitro translation assay proved compound 10 was able to potently inhibit protein synthesis of *E. coli* 70 S ribosome[38]. We hypothesize the bacterial 70 S ribosome as a possible intracellular target of TD-H2-A.

Most notably, we discovered that, in the TD-H2-A-treated group, the most significantly downregulated gene was *ndk*(46.7-fold change). The *ndk* gene encodes the diphosphate kinase, which is in charge of keeping the intracellular pool of nucleoside triphosphate (NTP) stable[39]. NTPs are essential for microbial growth, signal transduction, and pathogenicity[40]. Datas indicate that it is a critical novel host-responsive gene required for coordinating the virulence of *P. aeruginosa* during acute infection[41]. Therefore, it is worthwhile to investigate whether *ndk* has a similar function in *S. aureus*. We are currently constructing mutant strains of *S. aureus ndk* for further investigation.

In summary, our results demonstrated that the antibacterial mechanism of TD-H2-A might be a multitarget mode that affects several molecular pathways in *S. aureus* (Fig. 8), suggesting that it is a promising candidate for developing a new antimicrobial agent.

Materials and methods

Bacterial strains and compounds

S. aureus ATCC 35,556 was donated by the Department of Infection Biology (University of Tubingen, Germany). The compound used in this study (TD-H2-A; the purity was 95%) was dissolved in dimethyl sulfoxide (DMSO; Amresco, USA) up to 5 mM for use as a stock solution. TD-H2-A was designed and produced in cooperation with Nanjing Tech University. (Refer to the Supplementary Materials for further details on TD-H2-A).

Scanning electron microscopy (SEM)

An overnight culture of *S. aureus* ATCC 35,556 was inoculated into polystyrene 24-well plates, and incubated for 6–48 h. Then DMSO, vancomycin (10 μg/mL) or 5×MIC TD-H2-A were added into each well, and incubated for 16 h. The cells were fixed with 2.5% glutaraldehyde at 4 °C for at least 12 h and then washed three times with PBS. Samples were fixed with 1% osmic acid solution. After aspiration and discarding osmic acid solution, the samples were rinsed again three times with 0.1 M, pH 7.0 PBS solution for 15 min each time. Dehydration

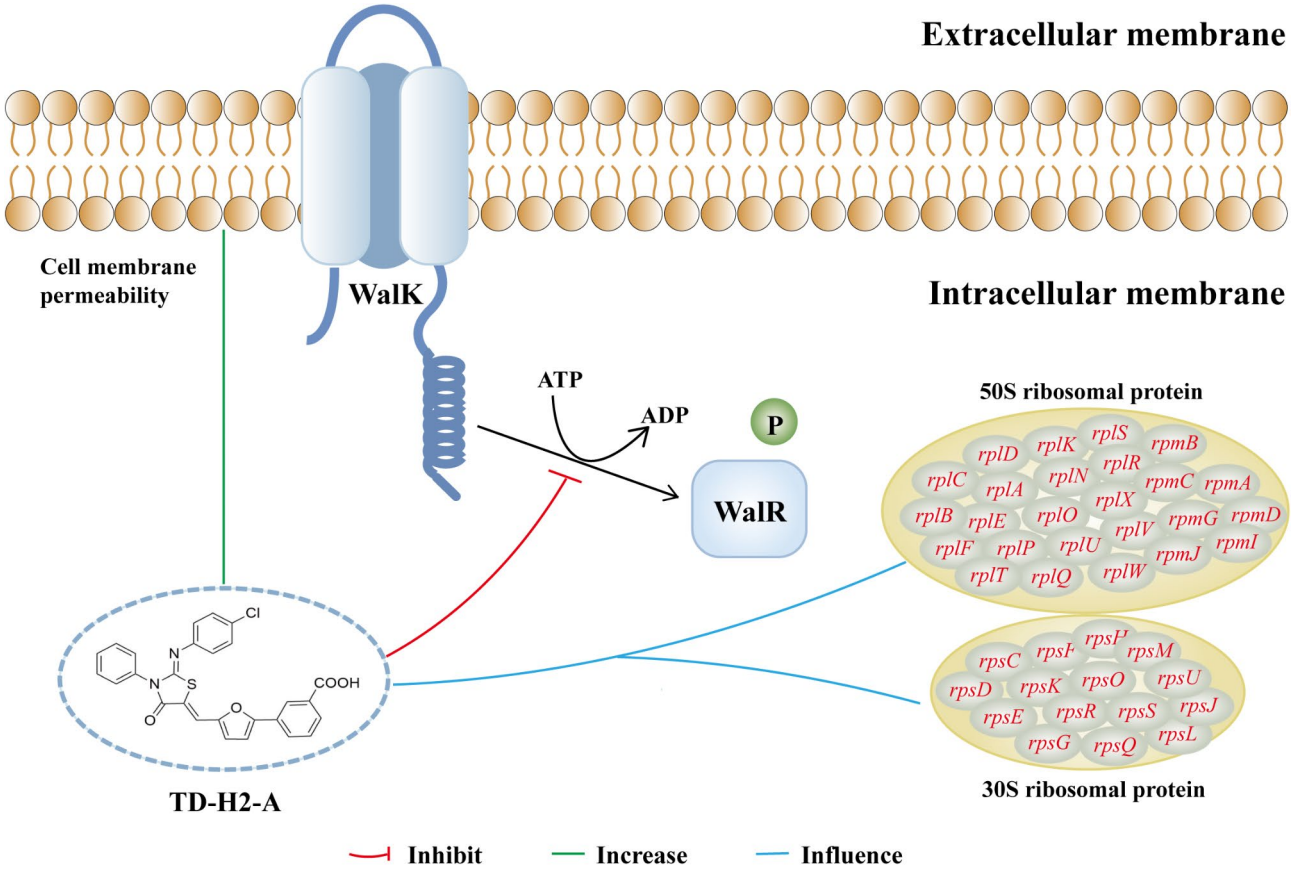

Fig. 8. Illustration of the antimicrobial mechanism of TD-H2-A.

was carried out with 30%, 50%, 70%, 80%, 90%, 95% and 100% ethanol sequentially with 10 min each time. After drying, the plates were plated with gold and examined under a scanning electron microscope [JSM-7900 F (JEOL)].

Inhibition assay for walk protein autophosphorylation

WalK (Lys208-Glu608) protein with an N-His tag was purchased from Wuhan Chemstan Biotechnology Co., Ltd. The inhibitory activities of the compound TD-H2-A on the ATPase activity of the WalK protein were measured by using the Kinase-Lumi™ Luminescent Kinase Assay Kit (Beyotime Co., Ltd., Nanjing, China). Briefly, 4 μg of purified WalK protein was preincubated with a series of dilutions of TD-H2-A in a reaction buffer (40 mM Tris, 20 mM $MgCl_2$, and 0.1 mg/mL BSA, pH 8.0) at 25℃ for 30 min, then 4 μM ATP was added and incubated for 30 min at room temperature, after which the Luminescent Kinase Reagent was added to detect the remaining amount of ATP, as reflected by the luminescence intensity (RLU). In parallel, WalK protein, with no addition of TD-H2-A, was used as the control, while ATP alone was used as a blank. The rate of inhibition of protein phosphorylation (Rp) by TD-H2-A was calculated using the following equation:

$$\mathrm{Rp} = \frac{\mathrm{RLU\,(Protein + compound + ATP + Reagent)} - \mathrm{RLU\,(Protein + ATP + Reagent)}}{\mathrm{RLU\,(ATP + Reagent)} - \mathrm{RLU\,(Protein + ATP + Reagent)}} \times 100\%$$

The 50% inhibition concentration (IC50) values for TD-H2-A inhibition of WalK protein phosphorylation were obtained by using GraphPad Prism 10.

RNA-seq analysis

S. aureus ATCC 35,556 strain was cultured in TSB at 37 °C for 12 h. The abovementioned overnight culture of *S. aureus* ATCC 35,556 strain was inoculated at 1:100 in 3 mL of TSB medium. After approximately 4 h of 37 °C 200 rpm shaking incubation (OD_{600} = 0.6–0.8), 1× MIC TD-H2-A was added for 15 min. For the negative control, the bacteria were inoculated in 1% DMSO. Three biological repeated samples were prepared for each strain. RNA-seq was performed by Personalbio Co., Ltd. (Nanjing, China). The number of successful reads was quantified and assessed by Personalbio Co., Ltd. The DEGs were analyzed by the software DESeq.

We used DESeq for differential analysis of the gene expression and screened the DEGs in the following ways: expression difference multiple $|\mathrm{Log_2FoldChange}| > 1$, significant $P < 0.05$. The volcano map of DEGs was plotted by the ggplots2 software package in R language. GO enrichment analysis of DEGs was performed using the R package topGO. The list of genes and the number of genes were calculated for each term using the GO term-

Gene	Primer
ndk	Forward 5'- TGGAACTTGCTGAAACACATTATGG – 3'
	Reverse 5'- TTGCGAACACTGGTGCTGATG – 3'
ugpC	Forward 5'- ATATGGCATTTGGGCTAAAGCTACG – 3'
	Reverse 5'- TGACGCTGTCCACCAGATAACG – 3'
gntK	Forward 5'- GTTTGTTATTGGTGCGAGTGATGGG-3'
	Reverse 5'- GTACCGATTGTGACAGCAACTTCTC – 3'
sdpB	Forward 5'-GCACTCACAATTGCAGCTTACATAG-3'
	Reverse 5'- TGCGCCAATCCCAATCGTATATG-3'
ftsL	Forward 5'-TGCGCCAATCCCAATCGTATATG-3'
	Reverse 5'- CATCCCCTGTTTCTTAGCCTTTTCG – 3'
ytkD	Forward 5'- CAGCAGGGCCAGTGTTGTTTAAC-3'
	Reverse 5'- ATCCAAGTGATTGCACCCTCTCTAC-3'
sdrC	Forward 5'- AAGTGGTCATGAAGCTAAAGCGGC – 3'
	Reverse 5'- CTGATCTGCAGTTGCAGTTTGCGT-3'
sdrD	Forward 5'- GCAGATGGTGGCGAAGTTGACG – 3'
	Reverse 5'- CACTGTCTGAGTCTGAGTCGCTGT-3'
vraD	Forward 5'- CCAACAGGCGCACTCGACTC – 3'
	Reverse 5'- GCTGCAACCGGATCATGTGTAAC – 3'
vraE	Forward 5'- AAACGCATAGGCTTTACGCATACAG – 3'
	Reverse 5'- AATGCTATTGCGGCGAATACTGC – 3'
gyrB	Forward 5' CCAGGTAAATTAGCCGATTGC – 3'
	Reverse 5'ATCGCCTGCGTTCTAGAGTC-3'

Table 2. Primer sequences for quantitative RT-PCR.

annotated differential genes. Then, the P-value (significant enrichment was defined as $P<0.05$) was calculated by using a hypergeometric distribution method to identify the GO terms that were significantly enriched for the differential genes relative to the whole genomic background so as to determine the main biological functions performed by DEGs. Based on the KEGG enrichment analysis[42–44] of the differentially expressed genes, the top 20 pathway with the p-value minimum that is the most significant enrichment were selected for display.

qRT-PCR

S. aureus ATCC 35,556 strain was cultured in TSB at 37 °C for 12 h. The abovementioned overnight culture of *S. aureus* ATCC 35,556 strain was inoculated at 1:100 in 3 mL of the TSB medium. After approximately 4 h of shaking incubation at 37 °C and 200 rpm, 1×MIC TD-H2-A was added and incubated for 15 min. Tubes containing bacteria inoculated with 1% DMSO served as control. RNA extraction was performed according to the manufacturer's instructions (EASYspin Plus Bacterial RNA Rapid Extraction Kit, Proteinbio, Nanjing). Next, extracted RNA (1 μg of each) was used as the template for cDNA synthesis by using the TRUEscript RT MasterMix (OneStep gDNA Removal) (Proteinbio). qRT-PCR was performed by using the SYBR Green II (Proteinbio) and Roche LightCycler®480 Fluorescence quantitative PCR instrument. The primer pairs used for qRT-PCR are listed in Table 2, with *gyrB* as the endogenous gene. The data were analyzed using a previously described relative quantitative ($2^{-\Delta\Delta Ct}$), fold changes in the gene expression were calculated, and the RNA transcription levels of biofilm-related genes were obtained. Three biological replicates and three technical replicates were performed for each gene tested.

Data availability

All data generated or analysed during this study are included in this published article. The RNA sequencing data can be found at PRJNA1154930 from Sequence Read Archive (SRA, https://www.ncbi.nlm.nih.gov/sra).

Received: 13 August 2024; Accepted: 14 March 2025
Published online: 26 March 2025

References

1. Ahmad-Mansour, N. et al. *Staphylococcus aureus* toxins: an update on their pathogenic properties and potential treatments. *Toxins (Basel)* **13**, 677. https://doi.org/10.3390/toxins13100677 (2021).
2. Guo, Y., Song, G., Sun, M., Wang, J. & Wang, Y. Prevalence and therapies of antibiotic-resistance in *Staphylococcus aureus*. *Front. Cell. Infect. Microbiol.* **10**, 107. https://doi.org/10.3389/fcimb.2020.00107 (2020).
3. Cabrera, R. et al. Molecular characterization of methicillin-resistant *Staphylococcus aureus* clinical strains from the endotracheal tubes of patients with nosocomial pneumonia. *Antimicrob. Resist. Infect. Control* **9**, 43. https://doi.org/10.1186/s13756-020-0679-z (2020).
4. Chen, Y. et al. Epidemiology, evolution and cryptic susceptibility of methicillin-resistant *Staphylococcus aureus* in China: a whole-genome-based survey. *Clin. Microbiol. Infect.* **28**, 85–92. https://doi.org/10.1016/j.cmi.2021.05.024 (2022).

5. Howden, B. P. et al. *Staphylococcus aureus* host interactions and adaptation. *Nat. Rev. Microbiol.* **21**, 380–395. https://doi.org/10.1038/s41579-023-00852-y (2023).
6. Lister, J. L. & Horswill, A. R. *Staphylococcus aureus* biofilms: recent developments in biofilm dispersal. *Front. Cell. Infect. Microbiol.* **4**, 178. https://doi.org/10.3389/fcimb.2014.00178 (2014).
7. Moormeier, D. E. & Bayles, K. W. *Staphylococcus aureus* biofilm: a complex developmental organism. *Mol. Microbiol.* **104**, 365–376. https://doi.org/10.1111/mmi.13634 (2017).
8. Idrees, M., Sawant, S., Karodia, N. & Rahman, A. *Staphylococcus aureus* biofilm: morphology, genetics, pathogenesis and treatment strategies. *Int. J. Environ. Res. Public. Health*. **18**, 7602. https://doi.org/10.3390/ijerph18147602 (2021).
9. Hoffman, L. R. et al. Aminoglycoside antibiotics induce bacterial biofilm formation. *Nature* **436**, 1171–1175. https://doi.org/10.1038/nature03912 (2005).
10. Dubrac, S., Boneca, I. G., Poupel, O. & Msadek, T. New insights into the WalK/WalR (YycG/YycF) essential signal transduction pathway reveal a major role in controlling cell wall metabolism and biofilm formation in *Staphylococcus aureus*. *J. Bacteriol.* **189**, 8257–8269. https://doi.org/10.1128/JB.00645-07 (2007).
11. Villanueva, M. et al. Sensory deprivation in *Staphylococcus aureus*. *Nat. Commun.* **9**, 523. https://doi.org/10.1038/s41467-018-02949-y (2018).
12. Bleul, L., Francois, P. & Wolz, C. Two-Component systems of *S. aureus*: signaling and sensing mechanisms. *Genes (Basel)*. **13**, 34. https://doi.org/10.3390/genes13010034 (2021).
13. Aimee, R. T. & Philip, N. R. Roles of two-component regulatory systems in antibiotic resistance. *Future Microbiol.* **14**, 533–552. https://doi.org/10.2217/fmb-2019-0002 (2019).
14. Zhao, R. et al. Antimicrobial and anti-biofilm activity of a thiazolidinone derivative against *Staphylococcus aureus* in vitro and in vivo. *Microbiol. Spectr.* **12**, e0232723. https://doi.org/10.1128/spectrum.02327-23 (2024).
15. Wei, G. et al. Comparative transcriptomic and functional assessments of linezolid-responsive small RNA genes in *Staphylococcus aureus*. *mSystems* **5**, e00665-00619. https://doi.org/10.1128/mSystems (2020).
16. Martin, J. K. et al. A dual-mechanism antibiotic kills gram-negative bacteria and avoids drug resistance. *Cell* **181**, 1518–1532e1514. https://doi.org/10.1016/j.cell.2020.05.005 (2020).
17. Wu, S., Liu, Y., Lei, L. & Zhang, H. Virulence of methicillin-resistant *Staphylococcus aureus* modulated by the YycFG two-component pathway in a rat model of osteomyelitis. *J. Orthop. Surg. Res.* **14**, 433. https://doi.org/10.1186/s13018-019-1508-z (2019).
18. Poupel, O. et al. Transcriptional analysis and subcellular protein localization reveal specific features of the essential walkr system in . *PLoS One* **11**, e0151449. https://doi.org/10.1371/journal.pone.0151449 (2016).
19. Cloeckaert, A. et al. In vitro activity of novel glycopolymer against clinical isolates of multidrug-resistant *Staphylococcus aureus*. *PloS One*. **13**, e0191522. https://doi.org/10.1371/journal.pone.0191522 (2018).
20. DeLeo, F. R. et al. Evolution of multidrug resistance during *Staphylococcus aureus* infection involves mutation of the essential two component regulator walkr. *PLoS Pathog.* **7**, e1002359. https://doi.org/10.1371/journal.ppat.1002359 (2011).
21. Cameron, D. R. et al. Impact of daptomycin resistance on *Staphylococcus aureus* virulence. *Virulence* **6**, 127–131. https://doi.org/10.1080/21505594.2015.1011532 (2015).
22. Foster, T. J. et al. Surface proteins of *Staphylococcus aureus*. *Microbiol. Spectr.* **7**, 0046-2018 (2019).
23. Askarian, F. et al. The interaction between *Staphylococcus aureus* SdrD and Desmoglein 1 is important for adhesion to host cells. *Sci. Rep.* **6**, 22134. https://doi.org/10.1038/srep22134 (2016).
24. Cheung, A. et al. β-Neurexin is a ligand for the *Staphylococcus aureus* MSCRAMM SdrC. *PLoS Pathog.* **6**, e1000726. https://doi.org/10.1371/journal.ppat.1000726 (2010).
25. McCourt, J., O'Halloran, D. P., McCarthy, H., O'Gara, J. P. & Geoghegan, J. A. Fibronectin-binding proteins are required for biofilm formation by community-associated methicillin-resistant *Staphylococcus aureus* strain LAC. *FEMS Microbiol. Lett.* **353**, 157–164. https://doi.org/10.1111/1574-6968.12424 (2014).
26. Feuillie, C. et al. Molecular interactions and Inhibition of the Staphylococcal biofilm-forming protein SdrC. *Proc. Natl. Acad. Sci. U S A*. **114**, 3738–3743. https://doi.org/10.1073/pnas.1616805114 (2017).
27. Cuong Vuong, H. L., Saenz, Friedrich, G. & Otto, M. Impact of the Agr Quorum-Sensing system on adherence to polystyrene in *Staphylococcus aureus*. *J. Infect. Dis.* **182**, 1688–1693 (2000).
28. Peng, Q., Tang, X., Dong, W., Sun, N. & Yuan, W. A review of biofilm formation of *Staphylococcus aureus* and its regulation mechanism. *Antibiot. (Basel)* **12**, 12. https://doi.org/10.3390/antibiotics12010012 (2022).
29. Parsek, M. R. & Greenberg, E. P. Sociomicrobiology: the connections between quorum sensing and biofilms. *Trends Microbiol.* **13**, 27–33. https://doi.org/10.1016/j.tim.2004.11.007 (2005).
30. Beis, K. Structural basis for the mechanism of ABC transporters. *Biochem. Soc. Trans.* **43**, 889–893. https://doi.org/10.1042/BST20150047 (2015).
31. Palleja, A. et al. Roux-en-Y gastric bypass surgery of morbidly obese patients induces swift and persistent changes of the individual gut microbiota. *Genome Med.* **8**, 67. https://doi.org/10.1186/s13073-016-0312-1 (2016).
32. Wu, S., Yu, P. L., Wheeler, D. & Flint, S. Transcriptomic study on persistence and survival of Listeria monocytogenes following lethal treatment with Nisin. *J. Glob Antimicrob. Resist.* **15**, 25–31. https://doi.org/10.1016/j.jgar.2018.06.003 (2018).
33. Nigam, S. K. What do drug transporters really do? *Nat. Rev. Drug Discov.* **14**, 29–44. https://doi.org/10.1038/nrd4461 (2015).
34. López-Marqués, R. L. et al. Structure and mechanism of ATP-dependent phospholipid transporters. *Biochim. Biophys. Acta*. **1850**, 461–475. https://doi.org/10.1016/j.bbagen.2014.04.008 (2015).
35. Khakhina, S. et al. Control of plasma membrane permeability by ABC transporters. *Eukaryot. Cell* **14**, 442–453. https://doi.org/10.1128/ec.00021-15 (2015).
36. Lin, J., Zhou, D., Steitz, T. A., Polikanov, Y. S. & Gagnon, M. G. Ribosome-Targeting antibiotics: modes of action, mechanisms of resistance, and implications for drug design. *Annu. Rev. Biochem.* **87**, 451–478. https://doi.org/10.1146/annurev-biochem-062917-011942 (2018).
37. Zhang, L. et al. Ribosome-targeting antibacterial agents: advances, challenges, and opportunities. *Med. Res. Rev.* **41**, 1855–1889. https://doi.org/10.1002/med.21780 (2021).
38. Luo, G. et al. Human defensin-inspired discovery of peptidomimetic antibiotics. *Proc. Natl. Acad. Sci. U S A*. **119**, e2117283119. https://doi.org/10.1073/pnas.2117283119 (2022).
39. Sikarwar, J., Singh, J., Singh, T. P., Sharma, P. & Sharma, S. The mechanism of action of Lactoferrin–Nucleoside diphosphate kinase complex in combating biofilm formation. *Protein Pept. Lett.* **29**, 839–850. https://doi.org/10.2174/0929866529666220816160517 (2022).
40. Abou-Dobara, M. I. et al. Allyl Rhodanine Azo dye derivatives: potential antimicrobials target d-alanyl carrier protein ligase and nucleoside diphosphate kinase. *J. Cell. Biochem.* **120**, 1667–1678. https://doi.org/10.1002/jcb.27473 (2019).
41. Yu, H. et al. Ndk, a novel host-responsive regulator, negatively regulates bacterial virulence through quorum sensing in Pseudomonas aeruginosa. *Sci. Rep.* **6**, 28684. https://doi.org/10.1038/srep28684 (2016).
42. Kanehisa, M. & Goto, S. KEGG: Kyoto encyclopedia of genes and genomes. *Nucleic Acids Res.* **28**, 27–30. https://doi.org/10.1093/nar/28.1.27 (2000).
43. Kanehisa, M. Toward understanding the origin and evolution of cellular organisms. *Protein Sci.* **28**, 1947–1951. https://doi.org/10.1002/pro.3715 (2019).
44. Kanehisa, M., Furumichi, M., Sato, Y., Kawashima, M. & Ishiguro-Watanabe, M. KEGG for taxonomy-based analysis of pathways and genomes. *Nucleic Acids Res.* **51**, D587–D592. https://doi.org/10.1093/nar/gkac963 (2023).

Acknowledgements
We would like to express our sincere gratitude to Prof. Wuyuan Lu, Dr Chongbing Liao and Dr Tao Xu of of Fudan University for their help. We also thank the Wutai Lab Center of the Second Affiliated Hospital of Nanjing Medical University. This work was supported by the National Natural Science Foundation of China (grant no.81802071) and Open Subject youth program of Key Laboratory of Medical Molecular Virology (MOE/NHC/CAMS) of Fudan University (grant no. FDMV-2023004).

Author contributions
All authors contributed to conception and study design. B.D., F.X., H.X. and R.Z. contributed to investigation. B.D. performed to manuscript writing. B. D., F.X., H.X. R.Z. and T.Z. contributed to interpretation of data. S.H. performed to synthesis of the compound. D.B., Ye Fei. Zhu, T.Z. and Yan Feng. Zhao contributed to writing—review and editing. Yan Feng. Zhao provided scientific direction. All authors reviewed the manuscript and approved the submitted version.

Declarations

Competing interests
The authors declare no competing interests.

Additional information
Supplementary Information The online version contains supplementary material available at https://doi.org/10.1038/s41598-025-94571-4.

Correspondence and requests for materials should be addressed to T.Z., Y.Z. or Y.Z.

Reprints and permissions information is available at www.nature.com/reprints.

Publisher's note Springer Nature remains neutral with regard to jurisdictional claims in published maps and institutional affiliations.